A density functional theory study of carbon monoxide oxidation on the $Cu_3Pt(111)$ alloy surface: Comparison with the reactions on Pt(111) and Cu(111)

C. J. Zhang, R. J. Baxter, and P. Hu[a)]
School of Chemistry, The Queen's University of Belfast, Belfast, BT9 5AG, United Kingdom

A. Alavi
Department of Chemistry, University of Cambridge, Cambridge, CB2 1EW, United Kingdom

M.-H. Lee
Department of Physics, Tamkang University, Tamsui, 25137 Taiwan

Alloying metals is often used as an effective way to enhance the reactivity of surfaces. Aiming to shed light on the effect of alloying on reaction mechanisms, we carry out a comparative study of CO oxidation on $Cu_3Pt(111)$, Pt(111), and Cu(111) by means of density functional theory calculations. Alloying effects on the bonding sites and bonding energies of adsorbates, and the reaction pathways are investigated. It is shown that CO preferentially adsorbs on an atop site of Pt and O preferentially adsorbs on a fcc hollow site of three Cu atoms on $Cu_3Pt(111)$. It is also found that the adsorption energies of CO (or O_a) decreases on Pt (or Cu) on the alloy surface with respect to those on pure metals. More importantly, having identified the transition states for CO oxidation on those three surfaces, we found an interesting trend for the reaction barrier on the three surfaces. Similar to the adsorption energies, the reaction barrier on Cu_3Pt possesses an intermediate value of those on pure Pt and Cu metals. The physical origin of these results has been analyzed in detail. © *2001 American Institute of Physics.* [DOI: 10.1063/1.1395626]

I. INTRODUCTION

Alloying metals has long been exploited in industry as an effective way to enhance the reactivity of surfaces.[1–3] This leads very often to new materials whose properties are substantially changed with respect to pure metals. Good examples are the Cu–Pt alloys. It is well known that Cu is a catalyst with low reactivity for the elimination of CO by oxidation, because stable oxide phases are easily produced due to the high oxygen affinity for Cu. On the other hand, although Pt exhibits high performances for CO oxidation especially when the CO coverage is low, it suffers from an autoinhibition effect: The large affinity of Pt for CO gives oxygen relatively restricted access to the catalyst surface, thus reducing the reactivity. Interestingly, Cu–Pt alloys have emerged as a very useful alternative in industrial application for the oxidation of CO to CO_2.[4,5] Furthermore, recent experimental studies of CO oxidation on Cu modified Pt(111) surfaces also suggested[6–8] that there is an enhanced reactivity of the alloy surface compared to pure Pt. Due to the great technological and scientific interest in alloy catalysts, it is of fundamental importance to understand how alloying modifies the nature of the surfaces and as a result their role in reactivity and catalysis.

The modified surface reactivity of alloys has been broadly rationalized by the "ligand" effect (by perturbing the electronic structure of the surface) and by the "ensemble" effect (by changing the adsorption sites of the reactants).[9–11] However, a detailed picture of how these effects influence the reaction mechanism of CO oxidation on the Cu–Pt alloy is not clear. Recently, some investigations on the electronic properties of Cu–Pt systems have been carried out.[12,13] It has been observed that the presence of Pt atoms broadens the Cu d band. A few studies have been devoted to CO chemisorption on $Cu_3Pt(111)$.[14–18] One finds, in general, that CO prefers the atop side of Pt on $Cu_3Pt(111)$. However, there is some discrepancy concerning the bond strength of CO on pure metal surface and alloy. One theoretical study showed that the CO–Pt bond is stronger on $Cu_3Pt(111)$ than Pt(111).[18] However, this result was questioned by a recent vibrational spectra study of CO adsorption by Becker *et al.* who reported a decreased Co–Pt bond strength from Pt(111) to $Cu_3Pt(111)$.[16] That the CO–Pt bond is stronger on Pt than on $Cu_3Pt(111)$ was also suggested by a model Hamiltonian investigation.[17] Obviously, further study is required. In addition, we note that, to date, little attention has been paid to O adsorption on alloy surface. Furthermore, no theoretical study of CO oxidation reaction on $Cu_3Pt(111)$ has appeared. Therefore, aiming to shed light on the alloying effect on the adsorption behaviors of CO and O, and more importantly the reaction mechanism, we have performed a density functional theory (DFT) investigation on CO oxidation on $Cu_3Pt(111)$.

Pt and Cu are known to form a continuous series of face-centered cubic solid solutions with different ordered phases.[19] On the ordered $Cu_3Pt(111)$ surface the Pt atoms form a 2×2 structure and each Pt atom is surrounded by Cu

---

[a)]Author to whom correspondence should be addressed. Electronic mail: p.hu@qub.ac.uk
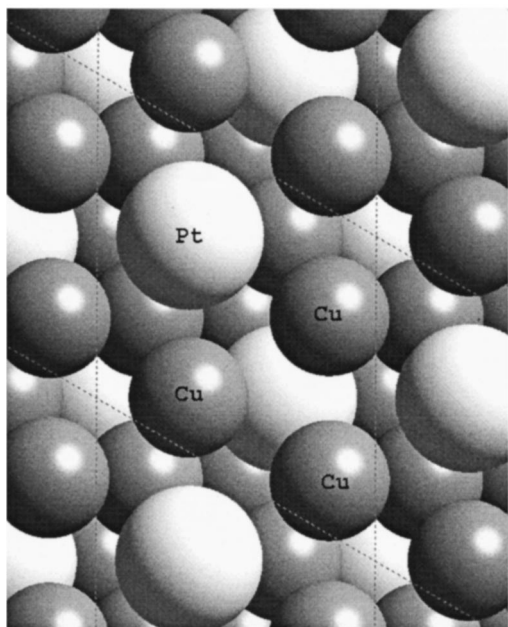
FIG. 1. Schematic structure for the pure $Cu_3Pt(111)$ surface. The $p(2\times2)$ unit cell is indicated in dotted lines.

atoms,[20] a schematic structure of which is shown in Fig. 1. We performed the DFT calculation on CO oxidation on the $Cu_3Pt(111)$ surface. The transition states (TSs) and the reaction barriers are determined. For comparison, we have also carried out the similar calculations for the reactions on Cu(111) and Pt(111). This paper is organized as follows: In Sec. II, the calculation details are outlined. In Sec. III A the most stable structure of CO and O adsorbed on $Cu_3Pt(111)$ is presented. A comparison of CO+O coadsorption structures among Cu(111), Pt(111), and $Cu_3Pt(111)$ is made, which leads to a discussion on the alloying effect on the adsorption properties. Following this, the TSs identified on three surfaces are presented and the alloying effect on the reaction pathway and the reactivity are analyzed. Finally, our conclusions are summarized in the last section.

II. CALCULATIONS

The DFT calculations were carried out with the generalized gradient approximation (GGA) for the exchange and correlated functional.[21,22] Ionic cores were described by ultrasoft pseudopotentials[23] and the Kohn–Sham one-electron states were expanded in a plane wave basis set up to 300 eV. A Fermi surface smearing of 0.1 eV was utilized to speed up the convergence of **k**-point sampling and the energy was extrapolated to 0 K of electronic temperature.[24,25] The supercell approach was employed to model periodic geometry. A $p(2\times2)$ unit cell was chosen in the calculations. The $Cu_3Pt(111)$, Pt(111), and Cu(111) surfaces were represented by three layer slabs of metal atoms separated by a vacuum region of 14 Å. The equilibrium lattice constants for $Cu_3Pt(111)$, Pt(111), and Cu(111) were calculated to be 3.7204 Å, 3.9771 Å, and 3.6234 Å, respectively, which are very close to the experimental data of ~3.69 Å for $Cu_3Pt(111)$,[26] 3.9236 Å for Pt,[27] and 3.6146 Å for Cu.[27] In

our calculations, the bottom two layers were held fixed in their calculated bulk positions, while the top layer of surface atoms was allowed to relax. A Monkhorst–Pack mesh[28] of $4\times4\times1$ **k**-grid was used to sample the surface Brillouin zone of the 2×2 supercell. As shown in recent work,[29–31] the above set up provides sufficient accuracy. In addition, convergence with respect to the cutoff energy and the number of slab layers has been checked using a 400 eV cutoff energy and four layers of metal atoms, respectively. It was found that the calculated structural differences are very small, typically being ~0.01 Å, and that the reaction barriers differ by less than 0.1 eV.

TSs were searched using a constrained optimization scheme.[29,32] In this approach, the distance between the C and the adsorbed O, labeled as O_a hereafter, was fixed and remaining degrees of freedom were optimized according to the forces calculated using Hellmann–Feynman theorem. The TS was identified when the following conditions were reached: (i) all forces on atoms vanish; and (ii) the total energy is a maximum with respect to the reaction coordinate and a minimum with respect to the remaining degrees of freedom.

III. RESULTS AND DISCUSSION

A. Alloying effect on the adsorption of CO and O_a

To examine the reaction mechanism, it is essential to understand the initial structure of the adsorbates on the surface. Structural optimizations were first performed on all possible high symmetry sites for CO and O_a coadsorption. It was found that in the most stable structure, the O_a sits on a fcc hollow site of three Cu atoms and the CO on an atop site of a Pt atom, as shown in Fig. 2(a). That the CO preferentially adsorbs on the atop site of Pt on Cu_3Pt surface is in accord with experimental studies on CO/$Cu_3Pt(111)$, including He II photoelectron spectra,[14] low energy He$^+$ ion scattering,[15] and high resolution electron energy loss spectroscopy.[16]

We also carried out structural optimizations for the coadsorption of CO and O_a on two pure metal surfaces, Pt(111) and Cu(111). In parallel to the $Cu_3Pt(111)$-$p(2\times2)$-(CO+Oa) system, similar (2×2) structures were set up for the coadsorption of CO and O_a on the pure metal surfaces. The Pt(111)-$p(2\times2)$-(CO+O_a) system is well characterized experimentally,[33] in which the O_a adsorbs on the fcc hollow site and the CO on the atop site. Our calculations are consistent with this structure, as shown in Fig. 1(b).[34] In the Cu(111)-$p(2\times2)$-(CO+O_a) system, our calculations reveal that the most stable structure is O_a being on the fcc hollow site and CO on the atop site, which is also consistent with the results of experimental studies on pure CO (Refs. 35,36) and pure O (Refs. 37,38) adsorptions on Cu(111). Interestingly, our calculations show that the initial structures for CO oxidation on three surfaces are very similar: On either the pure surfaces or the alloy surface, the CO and O_a always prefer an atop site and a fcc hollow site, respectively, in $p(2\times2)$ unit cells.

In Table I, we list the calculated chemisorption energies of CO and O_a on three surfaces, together with the data avail-
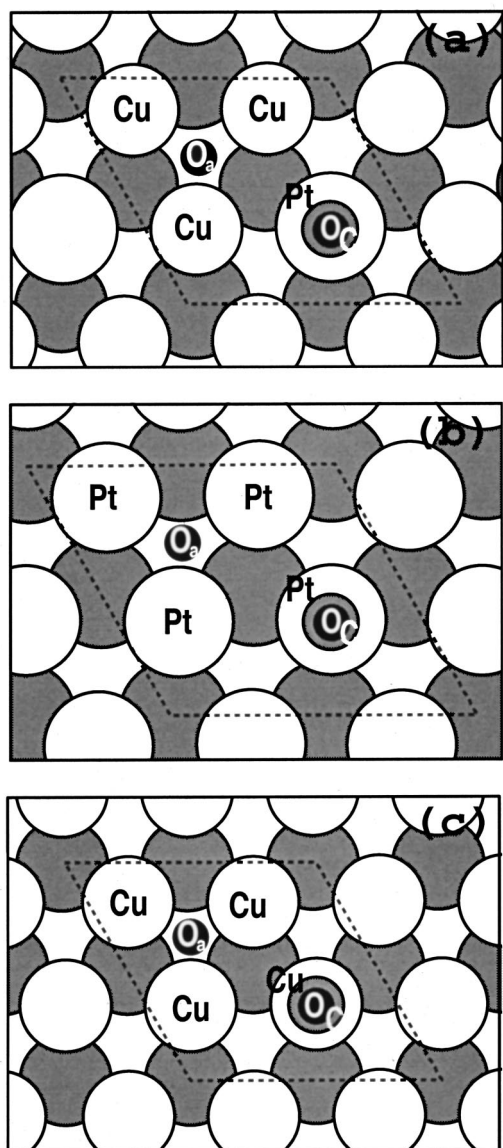
FIG. 2. Schematic structures for the coadsorption of CO and O_a on Cu$_3$Pt(111), Cu(111), and Pt(111).

able from the literature[17,18,39–45] (in the case of oxygen, the isolated oxygen atom is computed using a spin-polarized GGA). It can be seen that the agreement between our calculated results and the previously reported ones is good. The

results show that CO–Pt bond is significantly stronger than the CO–Cu bond, and conversely, the O–metal bond is stronger on Cu than that on Pt. There is a rich body of literature concerning CO and O_a adsorptions on Cu and Pt.[46–50] The strong bond of CO–Pt can be readily explained as follows: (i) the open d-shell nature of Pt permits a significantly bonding contribution from the orbital mixing between the 4σ, 5σ orbitals of the CO and the metal surface; and (ii) the extended $5d$ shell also facilitates the orbital mixing between the CO 2π and the metal surface. In Cu, by contrast, the full and contracted d-shell ($3d^{10}$) electronic configuration considerably reduce the bonding contribution from the 4σ and the 5σ orbitals of CO as well as the CO 2π orbitals, resulting in a weak CO–Cu bond. On the other hand, the relatively weak bond of O–Pt can be attributed to the antibonding nature of the $p(O)-d(Pt)$ states which exist below the Fermi level (E_f), and consequently weaken the O–Pt bond. In addition, the cohesive energy of Pt metals is larger than that of Cu metals, therefore, it is more difficult to break the Pt–Pt bond; Pt is generally more noble than Cu, less readily forming stable bonds with atoms such as H, C, N, and O.[51] Obviously, our results reflect the general consensus that Cu has a relatively large affinity for O, and Pt a relatively large affinity for CO. In fact, it is for this reason that, on the alloy surfaced, O prefers adsorption on the hollow site of three Cu atoms, and CO on the atop site of Pt.

We turn now to the effect of alloying on the adsorbate–metal bonding. Table I shows clearly that the CO–Pt and O–Cu bonds on the alloy surface are weaker than that on the corresponding pure metals. To understand these results, we calculated the local density of states (LDOS) projected onto a CO molecule in CO/Pt(111) and CO/Cu$_3$Pt(111) and LDOS projected onto an O_a atom in O_a/Cu(111) and O_a/Cu$_3$Pt(111), which are shown in Figs. 3(a) and 3(b), respectively. By examining the individual quantum states involved in the LDOS of CO [Fig. 3(a)], we found that the first peak from the left-hand side has a strong CO 3σ orbital character and the second one contains a CO 4σ character with a weak metal d-character. The third peak centered at ~7.7 eV below the E_f was found to be due to mixing of states with CO 1π and metal d-character, and the fourth peak at ~6.9 eV below E_f due to mixing of states with CO 5σ and metal d-character.[44,50] Comparison of the LDOS between CO/Pt(111) and CO/Cu$_3$Pt(111) shows that there is a slight

TABLE I. The calculated chemisorption energies of CO and O_a on Cu$_3$Pt(111), Cu(111), and Pt(111), together with the data available from literature.

	Chemisorption energy of CO (eV)		Chemisorption energy of O_a (eV)	
	This work	Literature	This work	Literature
Cu$_3$Pt(111)	1.51	1.42,[a] 1.51[b]	4.30	⋯
Pt(111)	1.59	1.45,[b] 1.50,[b] 2.23,[a] 1.55[d]	3.97	3.56,[f] 3.99,[f] 4.23,[g] 4.43[h]
Cu(111)	0.66	0.62,[b] 0.52,[e]	4.56	4.34–5.20[i]

[a]Reference 17.
[b]Reference 18.
[c]Reference 38.
[d]Reference 39.
[e]Reference 40.
[f]Reference 41.
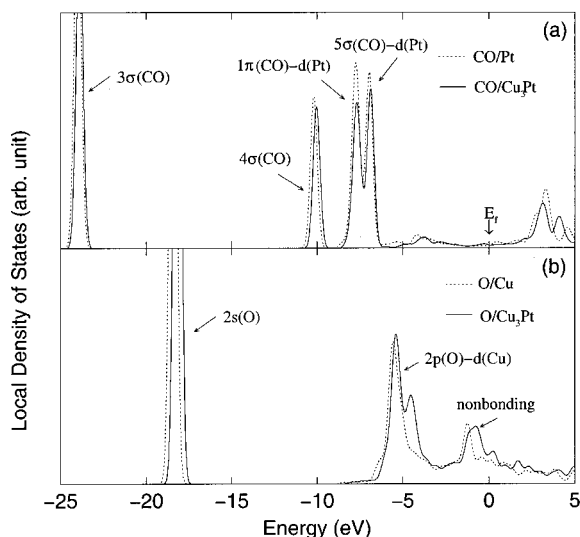[g]Reference 42.
[h]Reference 43.
[i]Reference 44.

FIG. 3. (a) Local density of states (LDOS) projected on a CO molecule in CO/Pt(111) and CO/Cu$_3$Pt(111); (b) LDOS projected on an O$_a$ atom in O/Pt(111) and O/Cu$_3$Pt(111).

FIG. 4. (a) Local density of states (LDOS) projected on a Cu atom in Cu(111) and Cu$_3$Pt(111); (b) LDOS projected on a Pt atom in Pt(111) and Cu$_3$Pt(111).

shift (less than 0.1 eV) towards higher energies in the LDOS in Cu$_3$Pt compared to that in Pt, which is accord with the result that the adsorption energy of CO decreases slightly from CO/Pt to CO/Cu$_3$Pt. This is also consistent with the photoemission characteristics observed on CO/Cu$_3$Pt(111) and CO/Pt.[14] For the LDOS of O, we see in Fig. 3(b), that the first peak contains exclusively the O 2s character and the second peak centered at −5 eV consists of strong mixing states between O 2p and Cu d orbitals, which is mainly responsible for the O–metal bonding. Examinations on the quantum states involved in the third peak centered at −2 eV in Fig. 3(b) show that the charge is highly accumulated around the O and little charge on metal atoms, and thus this peak has nonbonding character. These results agree well with the photoemission study on O/Cu(111):[52] Two peaks appear at 5.54±0.1 eV and 2.13±0.04 eV below the E_f. Compared to the LDOS on the pure Cu, a slight shift towards higher energies in the LDOS of O$_a$ on Cu$_3$Pt can be observed [Fig. 3(b)]. This is consistent with the result that the O–Cu bond in O/Cu(111) is stronger than that in O/Cu$_3$Pt(111). To understand further the origin of those features of LDOS, we calculated LDOS projected on metal atoms in pure and alloy surfaces. A comparison of LDOS projected on a Cu (or Pt) atom from the pure Cu (or Pt) and the Cu$_3$Pt(111) is shown in Fig. 4. There, it can be clearly seen that, upon alloying, the band center of Cu shifts towards a higher energy (by 0.42 eV) and the band center of Pt shifts towards a lower energy (by 0.12 eV). The shift of the Cu band increases the separation between the states of Cu and the p orbitals of O originally centered around 6.0 eV below the E_f, weakening the bonding interaction with the O. Consequently, it leads to a weaker O–CU bond in the alloy. On the other hand, the shift of the Pt and in the alloy towards lower energy [Fig. 4(b)] would reduce the contribution to the bonding between Pt d and CO 2π orbitals,[17,20] resulting in a weakened CO–metal bond. Interestingly, it can also be seen from our calculations (Table I) that the weakening of the CO–Pt bond from pure Pt
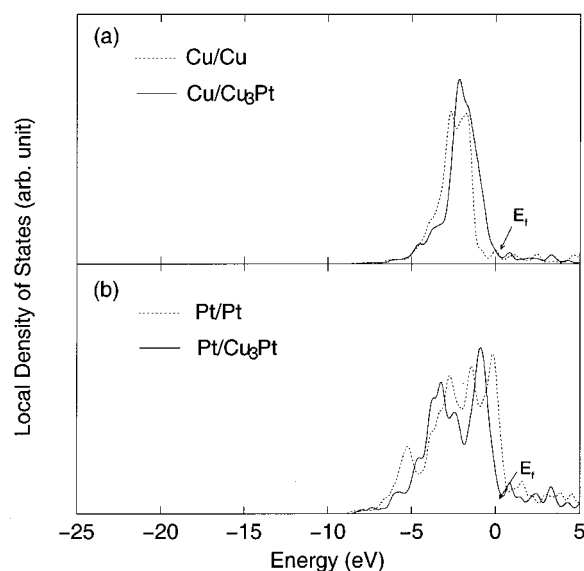
to Cu$_3$Pt is less than that of the O–Cu bond from pure Cu to Cu$_3$Pt.

B. Alloying effect on CO oxidation

Having determined the most stable co-adsorption structure of CO and O$_a$ on Cu$_3$Pt(111), the reaction pathways for CO oxidation have been searched. Two distinct TSs have been identified, which are schematically shown in Figs. 5(a) and 5(b). It can be seen that TS(a) is the structure with the O$_a$ being near a bridge site of two Cu atoms and CO being near an atop site of Pt and TS(b) is the structure with O$_a$ being near another bridge site of two Cu atoms and CO being near an atop site of Cu. The main structural parameters of the TSs are summarized in Table II. Relative to the most stable initial structure, the reaction barriers associated to TS(a) and TS(b) are calculated to be 0.80 eV and 1.40 eV, respectively.

We also carried out the calculations to investigate the reaction pathways on Cu(111) and Pt(111). As discussed in the last section, the adsorption of CO and O$_a$ on Cu$_3$Pt(111), Pt(111), and Cu(111) possess similar structures: The CO on an atop site and the O$_a$ on a fcc hollow site, which implies that the reaction paths might be similar on these surfaces. Indeed, a shown in Figs. 5(c), 5(d), 5(e), and 5(f), similar TSs are located on two pure metal surfaces. On both Pt(111) and Cu(111), the O$_a$ is very close to bridge sites with the CO slightly off the top sites, tilting away from the O$_a$ atoms. The main structural parameters of these TSs are also listed in Table II. With regard to CO oxidation on Pt(111), similar DFT calculations to search a TS as shown in Fig. 5(d) have been performed previously.[29] The results obtained in this study including the TS structure and the reaction barrier are in good agreement with those reported. It should be stressed that in contrast to Pt(111), experimentally the oxygen-covered Cu(111) surface tends to be reconstructed and the oxidized Cu(111) is easily formed,[53] which will result in a
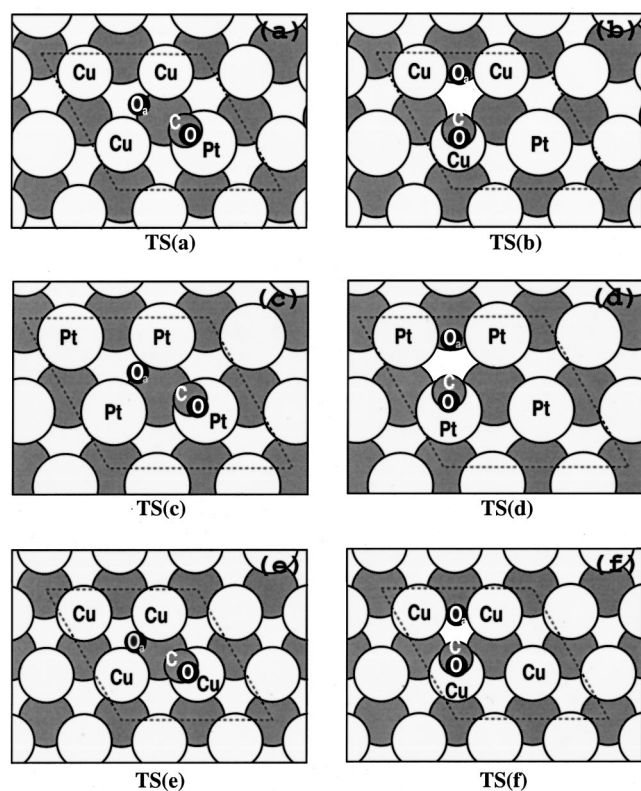
FIG. 5. Schematic structures for the TSs identified on Cu$_3$Pt(111), Cu(111), and Pt(111).

different reaction mechanism. However, in this study no reconstruction is considered for Cu(111), in order to make a comparison between the reaction pathways of Cu(111) and Cu$_3$Pt(111).

Table II also lists the calculated barriers for CO oxidation on these surfaces. It can be clearly seen that the barrier on Pt is the highest, the barrier on Cu is the lowest, and the barrier on the alloy surface represents an intermediate value, although the difference between them is very small. It is interesting to note that similar to the trend of the reaction barriers, both CO chemisorption energy and O chemisorption energy on Cu$_3$Pt also represent some intermediate between those of pure Cu and pure Pt.

TABLE II. The main structural parameters of the TSs identified on Cu$_3$Pt(111), Cu(111), and Pt(111) and the corresponding reaction barriers.

	C-metal (Å)	C–O (Å)	O$_a$–metal[a] (Å)	C–O$_a$ (Å)	Barrier (eV)
Cu$_3$Pt(111)					
TS(a)	1.99	1.17	1.92,1.94,2.16	1.80	0.80
TS(b)	1.84	1.15	1.89,1.89,2.53	1.98	1.40
Pt(111)					
TS(c)	1.93	1.16	2.08,2.09,2.92	1.96	0.87
TS(d)	1.90	1.15	2.026,2.06,2.87	2.10	0.85
Cu(111)					
TS(e)	1.94	1.17	1.91,1.92,2.18	1.72	0.68
TS(f)	1.88	1.16	1.85,1.85,2.45	1.90	0.71

[a]Three distances between O$_a$ and its nearest neighbors are listed.

To understand further the trend of the results described above, it is necessary to find out the physical origin of the reaction barrier. In our previous work,[29–31] we have determined two distinct reaction pathways for CO oxidation on Pt(111) and Ru(0001). The following common features have been observed. First, the CO molecule moves quite freely from its initial top site, with little energy change, while the O$_a$ vibrates around its threefold hollow position. Second, the O$_a$ becomes activated and moves to a bridge site to achieve the TS with the CO on an off-top site. During the second period, the energy changes dramatically. It was therefore concluded that the O$_a$ activation from a hollow site (usually the most stable site) to a bridge site is the most important step in the reaction. Since the TSs' structures obtained on Cu(111), Pt(111), and Cu$_3$Pt(111) in this study are very similar to those identified previously,[29–31] the similar reaction pathway features can be expected. However, it should be noted that CO is known to be mobile on the Pt(111) and Ru(0001) surface,[29,54,55] whereas the potential energy surface for CO diffusion is very corrugated on the alloy surface, as indicated in the large difference of the bond strength between CO–Cu and CO–Pt. Considering this, we suggest that two factors contribute significantly to the reaction barrier: (i) the O$_a$ activation; and (ii) the CO activation. In other words, the reaction barrier is determined by the energy changes caused by the activation of both species from the initial state to the TS. To illustrate this, taking TS(a), TS(c), and TS(e) identified on the three surfaces as examples, we carried out the following analysis. We calculated the individual energy change for O$_a$ (or CO) from the initial state to the TS without CO (or O$_a$) in each case. For example, the energy change of the O$_a$ chemisorption from the initial state to the TS refers to the chemisorption energy difference between the O$_a$ in a structure identical to the initial state of the reaction but without the CO and the O$_a$ in a structure identical to the TS without CO. The energy change of the CO movement was calculated in a similar manner. We found that the O$_a$ movement on Pt(111) costs the largest energy, being about 0.63 eV, whereas the energy losses for the O$_a$ movement on Cu(111) and Cu$_3$Pt(111) are relatively small, being about 0.47 eV and 0.38 eV, respectively. Furthermore, we found that the energy change for CO activation from an atop site in the initial state to an off-top site in the TS is in the order of Cu$_3$Pt(111)>Pt(111)≈Cu(111). On Cu(111) and Pt(111), due to the relatively flat potential energy surfaces for CO–metal interaction, the energy changes for CO movements are relatively small, being about 0.18 eV and 0.23 eV, respectively. On the other hand, the potential energy surface of CO on the alloy surface is strongly corrugated, this effect originating from a large difference between CO–Cu and CO–Pt bond strength. The energy loss, therefore, for CO movement from the initial state to TS has a large value, being approximately 0.52 eV. Taking these two factors into account, it is therefore expected that the barrier for the reaction on Cu(111) should be slightly lower, and the barrier on Pt(111) and Cu$_3$Pt(111) should be similar, which is consistent with the determined barriers in Table II. Similar features are also expected for the second reaction pathway, which is associated with the TS(d) or TS(f), except in the case of Cu$_3$Pt. The barrier associated

J. Chem. Phys., Vol. 115, No. 11, 15 September 2001

A density functional theory study of CO on Cu$_3$Pt(111)   5277

with TS(b) [Fig. 5(b)] is much higher than the corresponding values from the two pure metal surfaces. This is largely because in TS(b) on the alloy surface, the CO diffuses from an atop site of Pt to an atop site of a neighboring Cu, which contributes considerably to the high barrier.

IV. CONCLUSION

In summary, we have carried out a systematic study of CO oxidation on Cu$_3$Pt(111), Cu(111), and Pt(111) by means of DFT calculations. The alloying effect on adsorption sites of CO and O$_a$, bonding energies of CO and O$_a$ and the reaction mechanism have been shown and discussed. It is found the absorption energies of CO (or O$_a$) decreases on Pt (or Cu) on the alloy with respect to those on the pure metals. More importantly, by determining the TSs, we found that the reaction barrier on the alloy surface represents an intermediate value of those calculated from pure metals, although the difference between them is small. This implies that the Cu$_3$Pt alloy might be an even better catalyst for CO oxidation than pure Pt, in particular, considering the prohibitively high cost of pure Pt catalyst. The physical origins for those results have been analyzed in detail. Compared to the reaction mechanisms on pure metal surfaces, in which the O$_a$ activation is usually believed to be the most crucial step, a strong corrugated potential energy surface for the CO diffusion on the alloy surface leads to the CO activation from the initial state to the transition state being an important factor contributing to the reaction barrier.

ACKNOWLEDGMENTS

[1] V. Ponec, Catal. Rev. Sci. Eng. **11**, 1 (1975).

[2] C. T. Campbell, Annu. Rev. Phys. Chem. **41**, 775 (1990).

[3] U. Bardi, Rep. Prog. Phys. **57**, 939 (1994).

[4] J. T. Kunmmer, J. Catal. **38**, 166 (1975).

[5] H. C. de Jonstec and V. Ponec, J. Catal. **63**, 389 (1980).

[6] M. Kolodziejczyk, R. E. R. Colen, M. Berdau, B. Delmon, and J. H. Block, Surf. Sci. **375**, 235 (1997).

[7] M. Kolodziejczyk, R. E. R. Colen, B. Delmon, and J. H. Block, Appl. Surf. Sci. **121/122**, 480 (1997).

[8] R. E. R. Colen, M. Kolodziejczyk, B. Delmon, and J. H. Block, Surf. Sci. **412/413**, 447 (1998).

[9] J. H. Sinfelt, *Bimetallic Catalysis, Discoveries, Concepts, and Applications* (Wiley, New York, 1983).

[10] J. C. Bertolini, Surf. Rev. Lett. **3**, 1957 (1996).

[11] U. Schneider, H. Busse, R. Linke, G. R. Castro, and K. Wandelt, J. Vac. Sci. Technol. A **12**, 2069 (1994).

[12] B. Ginatempo, G. Y. Guo, W. M. Temmerman, J. B. Staunton, and P. J. Durham, Phys. Rev. B **42**, 2761 (1990).

[13] B. Hammer and J. K. Nørskov, Surf. Sci. **343**, 211 (1995).

[14] G. R. Castro, U. Schneider, H. Busse, T. Janssens, and K. Wandelt, Surf. Sci. **269–270**, 321 (1992).

[15] Y. G. Shen, D. J. O'Connor, K. Wandelt, and R. J. MacDonald, Surf. Sci. **331–333**, 746 (1995).

[16] C. Becker, T. Pelster, M. Tanemura, J. Breitbach, and K. Wandelt, Surf. Sci. **427–428**, 403 (1999).

[17] G. R. Castro and G. Doyen, Surf. Sci. **307–309**, 384 (1994).

[18] B. Hammer, Y. Morikawa, and J. K. Nørskov, Phys. Rev. Lett. **76**, 2141 (1996).

[19] M. Hansen and K. Anderko, *Constitution of Binary Alloys* (McGraw–Hill, New York, 1958).

[20] U. Schneider, G. R. Castro, H. Busse, T. Janssens, and K. Wandelt, Surf. Sci. **269/270**, 316 (1992).

[21] J. P. Perdew, Phys. Rev. B **33**, 8822 (1986); A. D. Becke, Phys. Rev. A **38**, 3098 (1988).

[22] M. C. Payne, M. P. Teter, D. C. Allen, T. A. Arias, and J. D. Joannopolous, Rev. Mod. Phys. **64**, 1045 (1992).

[23] D. Vanderbilt, Phys. Rev. B **41**, 7892 (1990).

[24] M. J. Gillan, J. Phys.: Condens. Matter **1**, 689 (1989).

[25] A. De Vita and M. J. Gillan, J. Phys.: Condens. Matter **3**, 6225 (1991).

[26] H. J. Monkhorst and J. D. Pack, Phys. Rev. B **13**, 5188 (1976).

[27] K. Mitsui, Y. Mishima, and T. Suzuki, Philos. Mag. A **53**, 447 (1986).

[28] D. R. Lide, *Handbook of Chemistry and Physics*, 78th ed. (CRC, London, 1998).

[29] A. Alavi, P. Hu, T. Deutsch, P. L. Silvestrelli, and J. Hutter, Phys. Rev. Lett. **80**, 3650 (1998).

[30] C. J. Zhang, P. Hu, and A. Alavi, J. Am. Chem. Soc. **121**, 7931 (1999).

[31] C. J. Zhang and P. Hu, J. Am. Chem. Soc. **122**, 2134 (2000).

[32] C. J. Zhang, P. Hu, and A. Alavi, J. Chem. Phys. **112**, 10564 (2000).

[33] J. Yoshinobu and M. Kawai, J. Chem. Phys. **103**, 3220 (1995).

[34] It should be noted that the atop site is not favored over the fcc hollow site for CO chemisorption on pure Pt(111) from DFT calculation, although the energy difference between these two sites is very small (0.1–0.2 eV) [see (a) P. J. Feibelman, J. Phys. Chem. B (in press); (b) M. Lynch and P. Hu, Surf. Sci. **458**, 1 (2000)]. In the present work we obtain the correct initial state of the reaction: We found from our calculations that the most stable structure for CO+O coadsorption in the $p(2\times2)$ unit cell is the CO on the atop site and the O on the fcc hollow site, which is consistent with experimental work. The reason for this is that in the $p(2\times2)$ unit cell the oxygen atom is bonded with three Pt atoms and there is only one free Pt atom left in the unit cell. The most stable site for CO chemisorption is, therefore, the top site of this Pt atom in order to avoid the so-called bonding competition (Refs. 29,44) with the O atom.

[35] S. Ishi, Y. Ohno, and B. Viswannathan, Surf. Sci. **162**, 349 (1985).

[36] J. C. Campuzano, *The Chemical Physics of Solid Surfaces and Heterogeneous Catalysis*, edited by D. A. King and D. P. Woodruff (Elsevier, Amsterdam, 1990).

[37] L. H. Dubois, Surf. Sci. **119**, 399 (1982).

[38] S. K. So, E. Franchy, and W. Ho, J. Chem. Phys. **95**, 1385 (1991).

[39] H. Steininiger, S. Lehwald, and H. Ibach, Surf. Sci. **123**, 264 (1982).

[40] P. H. T. Philipsen, E. van Lenthe, J. G. Snijders, and E. J. Baerends, Phys. Rev. B **56**, 13556 (1997).

[41] P. Hollins and J. Pritchard, Surf. Sci. **89**, 486 (1979).

[42] A. Kokalj, A. Lesar, and M. Hodošček, Chem. Phys. Lett. **268**, 43 (1997).

[43] A. Bogicevic, J. Strömquist, and B. I. Lundqvist, Phys. Rev. B **57**, R4289 (1997).

[44] K. Bleakley and P. Hu, J. Am. Chem. Soc. **121**, 7644 (1999).

[45] A. Mattsson, I. Panas, P. Siegbahn, U. Wahlgren, and H. Akeby, Phys. Rev. B **36**, 7389 (1987).

[46] F. Illas, S. Zurita, J. Rubio, and A. M. Marquez, Phys. Rev. B **52**, 12372 (1995).

[47] P. S. Bagus and F. Illas, Phys. Rev. B **42**, 10852 (1990).

[48] M. Chen, S. P. Bates, R. A. van Santen, and C. M. Friend, J. Phys. Chem. B **101**, 10051 (1997).

[49] A. Kokalj, A. Lesar, M. Hodošček, and M. Causà, J. Phys. Chem. B **103**, 7222 (1999).

[50] P. Hu, D. A. King, M.-H. Lee, and M. C. Payne, Chem. Phys. Lett. **246**, 73 (1995); P. Hu, D. A. King, S. Crampin, M.-H. Lee, and M. C. Payne, *ibid.* **230**, 501 (1994).

[51] B. Hammer and J. K. Nørskov, Nature (London) **376**, 128 (1995).

[52] D. Rieger, T. Wegehaupt, and W. Steinmann, Phys. Rev. Lett. **58**, 1135 (1987).

[53] J. Haase and H.-J. Kuhr, Surf. Sci. **203**, L695 (1988).

[54] A. A. Deckert, J. L. Brand, M. V. Arena, and S. M. George, Surf. Sci. **208**, 441 (1989).

[55] V. J. Kwasniewski and L. D. Schmidt, Surf. Sci. **274**, 329 (1992).